NUCL SCI TECH (2020) 31:59
https://doi.org/10.1007/s41365-020-00770-1

Multinucleon transfer dynamics in nearly symmetric nuclear reactions

Fei Niu[1] · Peng-Hui Chen[2,3] · Hui-Gan Cheng[1] · Zhao-Qing Feng[1]

Received: 6 March 2020 / Revised: 14 April 2020 / Accepted: 15 April 2020 / Published online: 27 May 2020

Abstract Within the framework of the dinuclear system model, the multinucleon transfer dynamics for nearly symmetric nuclear collisions has been investigated. The reaction mechanism in the systems of ^{198}Pt + ^{198}Pt and ^{204}Hg + ^{198}Pt was investigated at beam energies around the Coulomb barrier. It was found that the isotopic yields are enhanced with increased incident energy in the domain of proton-rich nuclides. However, the production on the neutron-rich side weakly depends on the energy. The angular distribution with the beam energy was also analyzed in the multinucleon transfer reactions. Projectile-like fragments were produced toward the forward emission with increasing incident energy. The target-like fragments manifested the opposite trend in the transfer reactions.

Keywords Dinuclear system model · Multinucleon transfer reactions · Symmetric nuclear collisions · Angular distribution

1 Introduction

The synthesis of new isotopes in the superheavy region is a key issue, motivated by extending the shell closure, discovering a new mechanism for nuclear fission, waiting point of nucleosynthesis during the r-process [1], quantum electrodynamics in strong Coulomb field, and more. Much progress has been made experimentally, and 3473 nuclides had been discovered as of 2018 [2]. Over 8000 nuclides might be bounded in a nuclear chart predicted by nuclear density functional theory [3]. There are several ways to create new isotopes in different mass domains, i.e., projectile fragmentation, fission of transactinide nuclei, fusion–evaporation mechanism, multinucleon transfer (MNT) reactions, etc. [4]. Up to now, the heavy-mass area with neutron number $N > 100$ is still blank and far from the neutron-drip line [5].

In recent years, the MNT mechanism near Coulomb barrier energies has been studied both experimentally and through different theoretical models, which provides a possible way to reach the heavy neutron-rich nuclei region. Theorists have developed some theoretical models to study MNT reactions, such as the dinuclear system (DNS) model [6–10], the GRAZING model [11, 12], and a dynamical model based on the Langevin equations [13, 14]. Furthermore, microscopic approaches based on the nucleon degree of freedom, the time-dependent Hartree–Fock (TDHF) approach [15–21], and the improved quantum molecular dynamics (ImQMD) model [22–24] have also been developed for describing the transfer reactions in nuclear collisions. Compared with other models, the DNS model can better consider the structural effects through the potential energy surface (PES), and the calculation time is short. In experiments, attempts to produce neutron-rich

This work was supported by the National Natural Science Foundation of China (Nos. 11722546 and 11675226) and the Talent Program of South China University of Technology.

✉ Zhao-Qing Feng
fengzhq@scut.edu.cn

[1] School of Physics and Optoelectronic Technology, South China University of Technology, Guangzhou 510641, China

[2] Institute of Modern Physics, Chinese Academy of Sciences, Lanzhou 730000, China

[3] University of Chinese Academy of Sciences, Beijing 100190, China

nuclei near $N = 126$ have been made through reactions of ^{136}Xe + ^{208}Pb or ^{64}Ni + ^{208}Pb at the Flerov Laboratory of Nuclear Reactions in Dubna [25], the Argonne National Laboratory [26], and the Helmholtz Centre for Heavy Ion Research (GSI) [27]. The neutron-rich isotopes via the MNT reaction ^{136}Xe + ^{198}Pt were also investigated at Grand Accélérateur National d'Ions Lourds (GANIL) in France [28]. Nearly symmetric reactions of massive nuclei, such as ^{204}Hg +^{198} Pt [29], also have been used to produce new neutron-rich isotopes at Argonne National Laboratory. Recently, the product yields in the MNT reaction for the system ^{204}Hg+^{208}Pb at both incident energies of 4.79 and 5.6 MeV/nucleon have been to test the models [30]. Modifications of the theoretical models are still needed to understand the experimental data. The inverse quasi-fission process occurs in nearly symmetric nuclear collisions, which provides a way to explore the competition of shape evolution and nucleon transfer dissipation and is helpful for modifying the theoretical models. The advantage of the DNS model over other models is the inclusion of structure effects in the nucleon transfer process, i.e., the shell and odd-even effects, fission heavy fragments, etc. However, the shape evolution is not considered in the DNS model, in which the individual properties of two fragments at the touching configuration are implemented. Nearly symmetric nuclear collisions will enlarge the shape effect on the observables, such as the fragment yields, energy spectra, and angular distribution. There are still some open problems in terms of transfer reactions, i.e., the mechanism of preequilibrium cluster emission, the mass limit of new isotopes with stable heavy target nuclides, the stiffness of the nuclear surface during the nucleon transfer process, etc.

In this work, the dynamical mechanism in MNT reactions of nearly symmetric systems was investigated with the DNS model. In Sect. 2, we give a brief description of the DNS model. Calculated results and discussion are presented in Sect. 3. A summary and perspective on the MNT reactions are presented in Sect. 4.

2 Brief description of the DNS model

The DNS concept was proposed by Volkov for describing the deep inelastic heavy-ion collisions near Coulomb barrier energies [31], where a few nucleon transfers were treated under the assumption of individual properties of DNS fragments. Application of the approach to superheavy nucleus formation via massive fusion reactions in competition with the quasifission process was used for the first time by Adamian et al. [32, 33]. The Lanzhou Group performed modifications of the relative motion energy and angular momentum of two colliding nuclei coupling to nucleon transfer within the DNS concept [34, 35], in which the nucleon transfer at the touching configuration of two colliding partners was coupled to the relative motion by solving a set of microscopically derived master equations. The contribution of quasi-fission and fission of heavy fragments was implemented in the nucleon transfer process. The dynamical mechanism in the fusion–evaporation and transfer reactions for producing the superheavy nuclei and exotic heavy nuclei was thoroughly investigated. Recently, the production cross sections of fragments in the MNT reactions around Coulomb barrier energies have been calculated using the DNS model [36, 37], particularly neutron-rich isotopes around the shell closure $N = 126$ and 162. The production cross sections of the MNT fragments were evaluated by

$$\sigma_{\rm tr}(Z_1,N_1,E_{\rm c.m.}) = \sum_{J=0}^{J_{max}} \sigma_{\rm cap}(E_{\rm c.m.},J) \int f(B) \times P(Z_1,N_1,E_1,J_1,B) \times W_{\rm sur}(E_1,J_1,s){\rm d}B. \quad (1)$$

Here, E_1 and J_1 denote the excitation energy and angular momentum for the DNS fragment (Z_1, N_1), respectively, which are the origin from the center of mass energy $E_{\rm c.m.}$ and the angular momentum J of the colliding system at the barrier B. The maximal angular momentum $J_{\rm max}$ corresponds to the grazing nucleus–nucleus collisions. The emission of γ rays and light particles in competition with binary fission is implemented in the evaluation of survival probability $W_{\rm sur}$ as a statistical model and s is the sum of evaporating particles, such as neutrons, protons, and α [38]. The capture cross section was calculated by the Hill–Wheeler formula with the barrier distribution approach [39]. The barrier distribution was taken as the Gaussian form $f(B) = \frac{1}{N}\exp[-((B - B_{\rm m})/\Delta)^2]$, with the normalization constant satisfying the unity relation $\int f(B){\rm d}B = 1$. The quantities $B_{\rm m}$ and Δ were evaluated by $B_{\rm m} = (B_{\rm C} + B_{\rm S})/2$ and $\Delta = (B_{\rm C} + B_{\rm S})/2$, respectively. $B_{\rm C}$ and $B_{\rm S}$ are the Coulomb barrier at waist-to-waist orientation and the minimum barrier from varying the quadrupole deformation parameters of the colliding partners.

The nucleon transfer is coupled to the relative motion energy and rotation energy. The time evolution of the probability $P(Z_1, N_1, E_1, t)$ for fragment 1 with proton number Z_1, neutron number N_1, and local excitation energy E_1 is described by the following master equations:

$$\begin{aligned}\frac{\mathrm{d}P(Z_1,N_1,E_1,t)}{\mathrm{d}t} &= \sum_{Z_1'} W_{Z_1,N_1;Z_1',N_1}(t)[d_{Z_1,N_1}P(Z_1',N_1,E_1',t) \\ &- d_{Z_1',N_1}P(Z_1,N_1,E_1,t)] \\ &+ \sum_{N_1'} W_{Z_1,N_1;Z_1,N_1'}(t)\times[d_{Z_1,N_1}P(Z_1,N_1',E_1',t) \\ &- d_{Z_1,N_1'}P(Z_1,N_1,E_1,t)].\end{aligned} \tag{2}$$

The mean transition probability $W_{Z_1,N_1;Z_1',N_1}(W_{Z_1,N_1;Z_1,N_1'})$ is calculated from the single-particle potential in valence space, and the microscopic dimension d_{Z_1,Z_1} is evaluated from the valence states and valence nucleons. We only include sequential nucleon transfer with the master equations by the relation of $Z_1' = Z_1 \pm 1$ and $N_1' = N_1 \pm 1$. The nucleons around the Fermi surface are active for transferring DNS fragments.

The local excitation energy E_1 is related to the dissipation energy of the relative motion and the potential energy surface (PES) of the DNS, which increases with relaxation time. The excitation energy at the equilibrium stage is distributed into the fragments according to mass. The angular momenta of the primary fragments are determined by the moment of inertia. The PES is evaluated by

$$\begin{aligned}U(\{\alpha\}) &= B(Z_1,N_1)+B(Z_2,N_2)-B(Z,N) \\ &+ V(\{\alpha\}),\end{aligned} \tag{3}$$

where Z and N are the proton and neutron numbers of the composite system, respectively; they satisfy the relations $Z_1+Z_2=Z$ and $N_1+N_2=N$. The symbol α represents the quantities of Z_1, N_1, Z_2, N_2, J, R, β_1, β_2, θ_1, and θ_2. The binding energies $B(Z_i,N_i)(i=1,2)$ and $B(Z,N)$ for the fragments and the compound nucleus (composite system without microscopic corrections for $Z>137$) are calculated by the droplet model. The ground-state quadrupole deformations β_i are considered in the calculation. The angles θ_i are the collision orientations for the deformed nuclei. The interaction potential $V(\{\alpha\})$ of the two DNS fragments is composed of nucleus–nucleus potential, Coulomb potential, and centrifugal force at the touching distance [6, 40].

Figure 1 shows the PES in the reaction ^{204}Hg $+^{198}$ Pt at the tip–tip orientation. The incident position of projectile and target nuclides is indicated by a pentagram in the chart. The occupation probability is dissipated from the entrance point to possible states once overcoming the local excitation energy. The pocket in the PES appears around the shell closure. The positive local excitation energy enables nucleon diffusion in the valence space. The structure effects of the fragment production in the MNT reactions are embodied in the PES. The low valley in the neutron-rich region is available for new isotope formation because of the large local excitation energy.

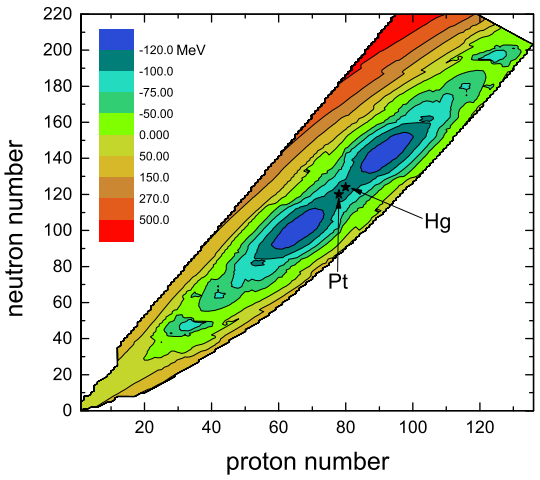

Fig. 1 (Color online) Potential energy surface of the DNS in the reaction ^{204}Hg $+^{198}$ Pt as a function of the protons and neutrons of the fragments

The emission angle of the MNT fragments is helpful for managing detectors in experiments, which is related to the reaction system and beam energy. We use a deflection function method to evaluate the fragment angle, where the fragment mass number, angular momentum, and local excitation influence the magnitude. The deflection angle is composed of the Coulomb and nuclear interaction as [41]

$$\Theta(l_i) = \Theta(l_i)_{\mathrm{C}} + \Theta(l_i)_{\mathrm{N}}. \tag{4}$$

The Coulomb scattering angle is given by the Rutherford function. The nuclear deflection angle is evaluated by

$$\Theta(l_i)_{\mathrm{N}} = \beta\Theta(l_i)_{\mathrm{C}}^{\mathrm{gr}}\frac{l_i}{l_{\mathrm{gr}}}\left(\frac{\delta}{\beta}\right)^{l_i/l_{gr}}, \tag{5}$$

where $\Theta_{\mathrm{C}}^{\mathrm{gr}}$ is the Coulomb scattering angle at the grazing angular momentum with $l_{\mathrm{gr}} = 0.22R_{\mathrm{int}}[A_{\mathrm{red}}(E_{\mathrm{c.m.}}-V(R_{\mathrm{int}}))]^{1/2}$. A_{red} and $V(R_{\mathrm{int}})$ correspond to the reduced mass of DNS fragments and interaction potential at the distance R_{int} from the entrance channel, respectively. δ and β are parameterized by fitting the deep inelastic scattering in massive collisions as

$$\begin{aligned}\beta &= 75f(\eta)+15, \quad \eta<375 \\ &\quad 36\exp(-2.17\times10^{-3}\eta), \quad \eta\geq375\end{aligned} \tag{6}$$

and

$$\begin{aligned}\delta &= 0.07f(\eta)+0.11, \quad \eta<375 \\ &\quad 0.117\exp(-1.34\times10^{-4}\eta), \quad \eta\geq375\end{aligned} \tag{7}$$

with

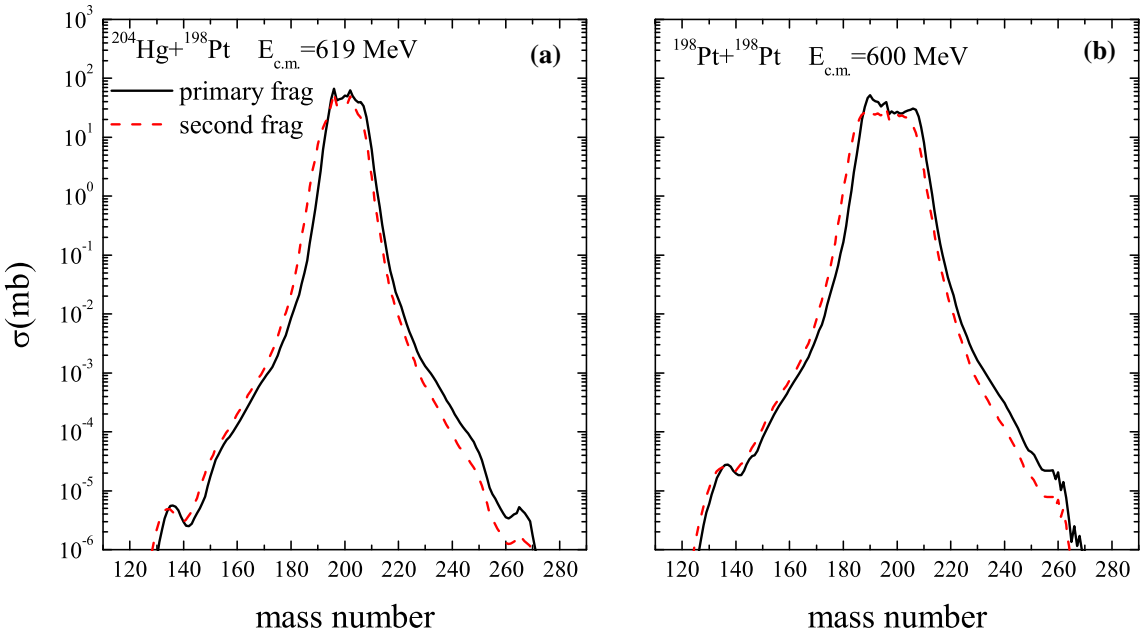

Fig. 2 (Color online) Cross sections as functions of the mass numbers of primary and surviving fragments in the reactions of **a** ^{204}Hg +^{198} Pt and **b** ^{198}Pt +^{198} Pt

$$f(\eta) = \left[1 + \exp\frac{\eta - 235}{32}\right]^{-1}, \tag{8}$$

where $\eta = \frac{Z_1 Z_2 e^2}{\upsilon}$, and $\upsilon = \sqrt{\frac{2}{A_{\text{red}}}(E_{\text{c.m.}} - V(R_{\text{int}}))}$.

3 The results and discussion

The primary fragments in MNT reactions must be de-excited to obtain the second fragments. This de-excitation process is described using a statistical model [38]. The cross sections that form fragments in this nuclear reaction can reflect the dynamics of a collision and the nuclear decay process of superheavy nuclei in excited states. Therefore, we can study these processes through cross sections. Figure 2 shows the cross sections of primary and secondary fragments formed by the MNT reactions of ^{204}Hg +^{198}Pt and ^{198}Hg +^{198}Pt. Due to the symmetry of the PES, the production cross sections of primary fragments (black lines) and second fragments (red lines)are nearly symmetric. The DNS dissipates into a broad mass region in the nuclear chart for primary fragments and approaches the neutron-rich domain. By comparing the distribution of the secondary fragment and the primary fragment formation cross sections with the mass number, it can be seen that the mass distribution of the secondary fragment formation cross section shifted to the left. This is because the primary fragment has a certain amount of excitation energy during the formation, and deactivation is reached. It should be noted that the production of heavy fragments ($m > 220$) decreased drastically with the mass number. This is due to the strong Coulomb repulsion inside the composite system, meaning the composite system can exist only for a short time of several tens of 10^{-22} s. The neck configuration is significant in symmetric damped collisions, which softens the potential barrier in the PES and is available for nucleon transfer [42, 43].

The calculated results were compared with the data from Argonne National Laboratory for the nearly symmetric system ^{204}Hg +^{198} Pt, as shown in Fig. 3. The production cross sections of bismuth in the MNT reactions were obviously underestimated by approximately two orders of magnitude in the calculations. It should be noted that the total cross section of all MNT fragments in experiments was larger than the geometric cross section (4.5 barn) owing to the lack of normalization in the thick target. Isotopic cross sections of projectile-like fragments (PLF) and target-like fragments (TLF) were measured at a beam energy of $E_{\text{c.m.}} = 619$ MeV close to the Coulomb barrier $V_{\text{C}} = 565$ MeV. The production cross sections of the transfer fragments were underestimated by 20 times the experimental data. Overall, the isotopic structure is con-

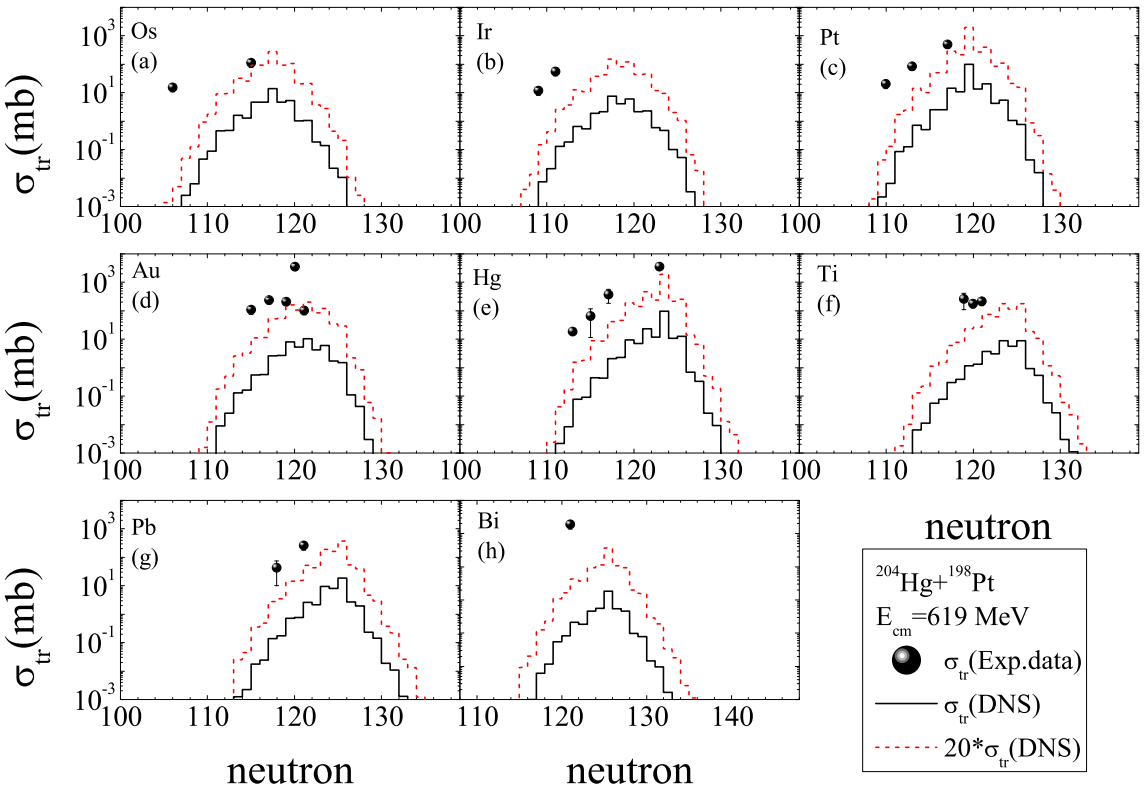

Fig. 3 (Color online) Isotopic distributions of MNT fragments in the reactions of ^{204}Hg $+^{198}$ Pt at the center of mass energy of 619 MeV compared with available data from Argonne [29]

sistent with the measurements but with narrow distributions. Inclusion of the shape evolution in the dissipation process might enlarge the nucleon transfer and enhance the production of MNT fragments away from the PLF or TLF regions, which is missed in the DNS model. This work is in progress.

The fragments formed in the symmetric or nearly symmetric transfer reactions undergo the inverse quasi-fission process. The nucleon transfer diffuses into enlarging the mass asymmetry under the PES. It provides the possibility for exploring the dissipation mechanism of two colliding heavy nuclei, stiffness of nuclear surfaces, superdeformation systems, new isotope production, etc. The transfer dynamics in the symmetric system were systematically investigated, as shown in Fig. 4 for the reaction of ^{198}Pt $+^{198}$ Pt near barrier energies. Four different energies were selected for the calculation, i.e., 500, 542, 570, and 600 MeV, in the center of mass frame of colliding nuclei. A narrow diffusion on the isotopic distribution is obvious at the sub-barrier energy ($V_C = 542$ MeV). On the proton-rich side, the transfer cross section increases with the incident energy. The energy dependence becomes slight in the neutron-rich region because high incident energy enhances the local excitation energy, which is favorable for nucleon transfer. There, the energy is higher than the Coulomb barrier, and more nuclei can cross the barrier to participate in the reaction and increase the probability of the reaction, so the cross sections of primary fragments increase with the energy. Meanwhile, the high local excitation energy leads to reduction in the survival probability of primary fragments. Both the mass drift and decay process of excited fragments contribute to secondary fragment formation. The fragments produced around the shell closure survive because of the larger separation energy. The beam energy should be selected close to the Coulomb barrier of the reaction system to measure the MNT fragments in experiments.

The anisotropy of fragment emission manifests the dynamical characteristics in MNT reactions, which is associated with deformation, dissipation of relative energy

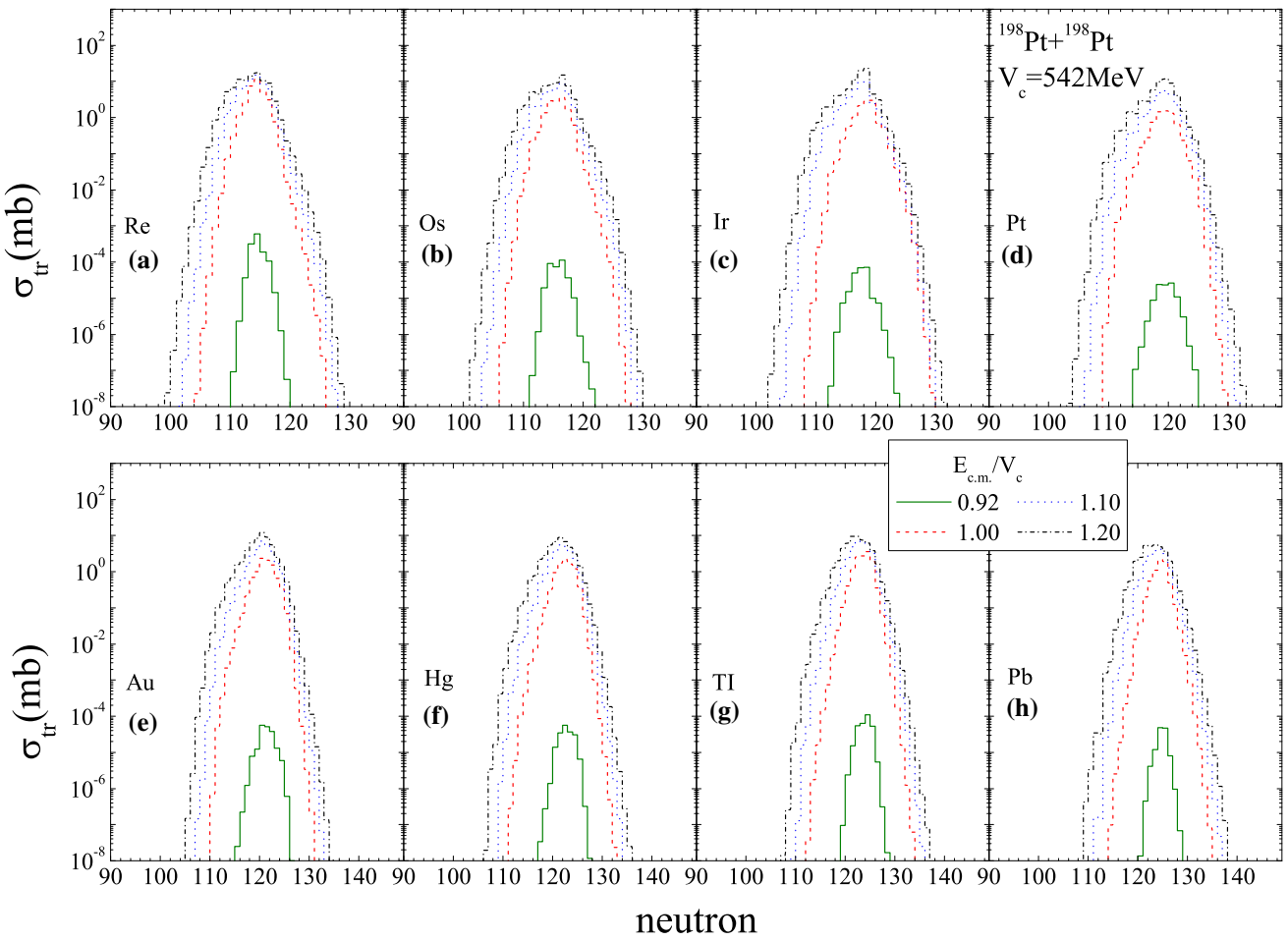

Fig. 4 (Color online) Incident energy dependence on the MNT fragments produced in the transfer reaction ^{198}Pt + ^{198} Pt

and angular momentum, configuration of nucleon transfer, etc. The shape of the angular distribution is an important criteria for the nuclear reaction mechanism. For example, the formation of a composite nucleus has a sufficiently long interaction time to allow the various degrees of freedom in the system to reach equilibrium, so the angular distribution of the reaction products appears to be 90° symmetrical in the center of mass. Estimation of the maximal yields from angular spectra of MNT fragments is beneficial for managing the detector system in experiments. Figure 5 shows the angular distributions of primary fragments of PLFs (black lines) and TLFs (red lines) in the damped collisions of ^{204}Hg + ^{198} Pt at the c.m. energies of 520, 580, 703 MeV. The PLFs tend to be emitted toward the forward direction with increasing beam energy. Opposite trends were found for the TLFs. A bump structure appears at high incident energy, which is around the Coulomb scattering angle. A broad distribution of MNT fragments is pronounced at the energy close to Coulomb barrier $V_C = 565$ MeV. The maximal yields of PLFs and TLFs correspond to 55° and 30°, respectively. The separation of the emission angle for PLFs and TLFs is enlarged with decreasing angular momentum of the colliding system.

4 Summary and conclusions

In summary, the dynamics in the MNT reactions around Coulomb barrier energies was investigated within the DNS model. The calculated isotopic distribution structure is consistent with the experimental data in the reaction of ^{204}Hg + ^{198} Pt. The maximal yields of fragments formed in the MNT reactions are located on the line of β stability. The isotopic cross sections are sensitive to the incident energy in the proton-rich region. The mass spectra of fragments in the symmetric system roughly exhibit a symmetric distribution, where the shell effect and odd–even effect contribute to the spectrum structure. The MNT fragments are produced in the forward-angle region along the colliding direction. The energy dependences of the

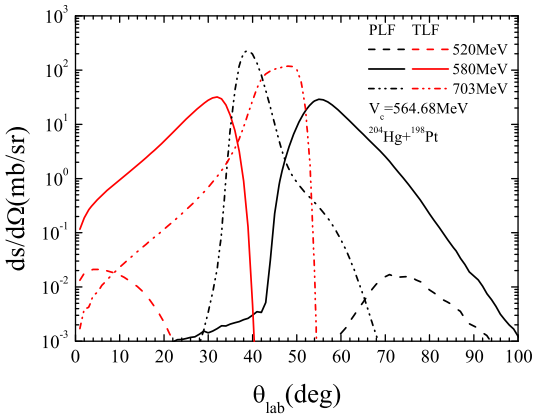

Fig. 5 (Color online) Angular distribution of Hg-like reaction products (black line) and Pt-like products (red line) in the laboratory frame

angular distributions for PLFs and TLFs are opposite. The MNT fragments are distributed in the narrow mass region, which might be caused by neglect of shape evolution in the nuclear dissipation. The couplings of more degrees of freedom, i.e., neck degree of freedom, mass asymmetry, elongation evolution, etc., need to be implemented. Further modifications are in progress.

References

1. M. Terasawa, K. Sumiyoshi, T. Kajino et al., New nuclear reaction flow during r-process nucleosynthesis in supernovae: critical role of light neutron-rich nuclei. Nucl. Phys. A **688**, 1–2 (2001)
2. M. Thoennessen, 2017 update of the discoveries of nuclides. Int. J. Mod. Phys. E **27**, 1830002 (2018). https://doi.org/10.1142/S0218301318300023
3. J. Erler, N. Birge, M. Kortelainen et al., The limits of the nuclear landscape. Nature (London) **486**, 509 (2012). https://doi.org/10.1038/nature11188
4. F. Niu, P.H. Chen, Y.F. Guo et al., Multinucleon transfer dynamics in heavy-ion collisions near Coulomb-barrier energies. Phys. Rev. C **96**, 064622 (2017). https://doi.org/10.1103/PhysRevC.96.064622
5. T. Kurtukian-Nieto, J. Benlliure, K.-H. Schmidt et al., Production cross sections of heavy neutron-rich nuclei approaching the nucleosynthesis r-process path around $A = 195$. Phys. Rev. C **89**, 024616 (2014). https://doi.org/10.1103/PhysRevC.89.024616
6. Z.Q. Feng, G.M. Jin, J.Q. Li, Production of new superheavy $Z = 108 - 114$ nuclei with ^{238}U, ^{244}Pu, and ^{248,250}Cm targets. Phys. Rev. C **80**, 057601 (2009). https://doi.org/10.1103/PhysRevC.80.057601
7. G.G. Adamian, N.V. Antonenko, V.V. Sargsyan et al., Possibility of production of neutron-rich Zn and Ge isotopes in multinucleon transfer reactions at low energies. Phys. Rev. C **81**, 024604 (2010). https://doi.org/10.1103/PhysRevC.81.024604
8. G.G. Adamian, N.V. Antonenko, V.V. Sargsyan et al., Predicted yields of new neutron-rich isotopes of nuclei with $Z = 64 - 80$ in the multinucleon transfer reaction ^{48}Ca+^{238}U. Phys. Rev. C **81**, 057602 (2010). https://doi.org/10.1103/PhysRevC.81.057602
9. G.G. Adamian, N.V. Antonenko, D. Lacroix, Production of neutron-rich Ca, Sn, and Xe isotopes in transfer-type reactions with radioactive beams. Phys. Rev. C **82**, 064611 (2010). https://doi.org/10.1103/PhysRevC.82.064611
10. X.B. Yu, L. Zhu, Z.H. Wu et al., Predictions for production of superheavy nuclei with $Z = 105 - 112$ in hot fusion reactions. Nucl. Sci. Tech **29**, 154 (2018). https://doi.org/10.1007/s41365-018-0501-2
11. A. Winther, Grazing reactions in collisions between heavy nuclei. Nucl. Phys. A **572**, 191 (1994). https://doi.org/10.1016/0375-9474(94)90430-8
12. A. Winther, Dissipation, polarization and fluctuation in grazing heavy-ion collisions and the boundary to the chaotic regime. Nucl. Phys. A **594**, 203 (1995). https://doi.org/10.1016/0375-9474(95)00374-A
13. V.I. Zagrebaev, W. Greiner, Cross sections for the production of superheavy nuclei. Nucl. Phys. A **944**, 257 (2015). https://doi.org/10.1016/j.nuclphysa.2015.02.010
14. D. Boilley, B. Cauchois, H. Lü et al., How accurately can we predict synthesis cross sections of superheavy elements? Nucl. Sci. Tech. **29**, 172 (2018). https://doi.org/10.1007/s41365-018-0509-7
15. C. Golabek, C. Simenel, Collision dynamics of two U-238 atomic nuclei. Phys. Rev. Lett. **103**, 042701 (2009). https://doi.org/10.1103/PhysRevLett.103.042701
16. C. Simenel, Particle-number fluctuations and correlations in transfer reactions obtained using the Balian–Vénéroni variational principle. Phys. Rev. Lett. **106**, 112502 (2011). https://doi.org/10.1103/PhysRevLett.106.112502
17. K. Sekizawa, K. Yabana, Time-dependent Hartree–Fock calculations for multinucleon transfer processes in^{40,48}Ca+^{124}Sn, ^{40}Ca+^{208}Pb, and ^{58}Ni+^{208}Pb reactions. Phys. Rev. C **88**, 014614 (2013). https://doi.org/10.1103/PhysRevC.88.014614
18. K. Sekizawa, K. Yabana, Phys. Rev. C **93**, 029902(E) (2016). https://doi.org/10.1103/PhysRevC.93.029902
19. L. Guo, C. Simenel, L. Shi et al., The role of tensor force in heavy-ion fusion dynamic. Phys. Lett. B **782**, 401–405 (2018). https://doi.org/10.1016/j.physletb.2018.05.066
20. X. Jiang, N. Wang, Production mechanism of neutron-rich nuclei around $N = 126$ in the multi-nucleon transfer reaction ^{132}Sn+^{208}Pb. Chin. Phys. C **42**, 104105 (2018). https://doi.org/10.1088/1674-1137/42/10/104105
21. K. Sekizawa, Microscopic description of production cross sections including deexcitation effects. Phys. Rev. C **96**, 014615 (2017). https://doi.org/10.1103/PhysRevC.96.014615
22. J. Tian, X. Wu, K. Zhao et al., Properties of the composite systems formed in the reactions of ^{238}U+^{238}U and ^{232}Th+^{250}Cf. Phys. Rev. C **77**, 064603 (2008). https://doi.org/10.1103/PhysRevC.77.064603
23. K. Zhao, Z. Li, X. Wu et al., Production probability of superheavy fragments at various initial deformations and orientations in the ^{238}U+^{238}U reaction. Phys. Rev. C **88**, 044605 (2013). https://doi.org/10.1103/PhysRevC.88.044605
24. K. Zhao, Z. Li, N. Wang et al., Production mechanism of neutron-rich transuranium nuclei in ^{238}U+^{238}U collisions at near-barrier energies. Phys. Rev. C **92**, 024613 (2015). https://doi.org/10.1103/PhysRevC.92.02461
25. E.M. Kozulin, E. Vardaci, G.N. Knyazheva et al., Mass distributions of the system ^{136}Xe+^{208}Pb at laboratory energies around the Coulomb barrier: a candidate reaction for the production of neutron-rich nuclei at $N = 126$. Phys. Rev. C **86**, 044611 (2012). https://doi.org/10.1103/PhysRevC.86.044611

26. J.S. Barrett, W. Loveland, R. Yanez et al., $^{136}Xe + ^{208}Pb$ reaction: a test of models of multinucleon transfer reactions. Phys. Rev. C **91**, 064615 (2015). https://doi.org/10.1103/PhysRevC.91.064615
27. O. Beliuskina, S. Heinz, V. Zagrebaev et al., On the synthesis of neutron-rich isotopes along the $N = 126$ shell in multinucleon transfer reactions. Eur. Phys. J. A **50**, 161 (2014). https://doi.org/10.1140/epja/i2014-14161-3
28. Y.X. Watanabe, Y.H. Kim, S.C. Jeong et al., Pathway for the production of neutron-rich isotopes around the $N = 126$ shell closure. Phys. Rev. Lett. **115**, 172503 (2015). https://doi.org/10.1103/PhysRevLett.115.172503
29. T. Welsh, W. Loveland, R. Yanez et al., Modeling multi-nucleon transfer in symmetric collisions of massive nuclei. Phys. Lett. B **771**, 119–124 (2017). https://doi.org/10.1016/j.physletb.2017.05.044
30. V.V. Desai, A. Pica, W. Loveland et al., Multinucleon transfer in the interaction of 977 MeV and 1143 MeV ^{204}Hg with ^{208}Pb. Phys. Rev. C **101**, 034612 (2020). https://doi.org/10.1103/PhysRevC.101.034612
31. V.V. Volkov, Deep inelastic transfer reactions. The new type of reactions between complex nuclei. Phys. Rep. **44**, 93 (1978). https://doi.org/10.1016/0370-1573(78)90200-4
32. G.G. Adamian, N.V. Antonenko, W. Scheid et al., Treatment of competition between complete fusion and quasifission in collisions of heavy nuclei. Nucl. Phys. A **627**, 361 (1997). https://doi.org/10.1016/S0375-9474(97)00605-2
33. G.G. Adamian, N.V. Antonenko, W. Scheid et al., Fusion cross sections for superheavy nuclei in the dinuclear system concept. Nucl. Phys. A **633**, 409 (1998). https://doi.org/10.1016/S0375-9474(98)00124-9
34. Z.Q. Feng, G.M. Jin, F. Fu, J.Q. Li, Production cross sections of superheavy nuclei based on dinuclear system model. Nucl. Phys. A **771**, 50 (2006). https://doi.org/10.1016/j.nuclphysa.2006.03.002
35. Z.Q. Feng, G.M. Jin, J.Q. Li, W. Scheid, Formation of superheavy nuclei in cold fusion reactions. Phys. Rev. C **76**, 044606 (2007). https://doi.org/10.1103/PhysRevC.76.044606
36. F. Niu, P.H. Chen, Y.F. Guo et al., Effect of isospin diffusion on the production of neutron-rich nuclei in multinucleon transfer reactions. Phys. Rev. C **97**, 034609 (2018). https://doi.org/10.1103/PhysRevC.97.034609
37. P.H. Chen, F. Niu, W. Zuo, Z.Q. Feng, Approaching the neutron-rich heavy and superheavy nuclei by multinucleon transfer reactions with radioactive isotopes. Phys. Rev. C **101**, 024610 (2020). https://doi.org/10.1103/PhysRevC.101.024610
38. P.H. Chen, Z.Q. Feng, J.Q. Li, H.F. Zhang, A statistical approach to describe highly excited heavy and superheavy nuclei. Chin. Phys. C **40**, 091002 (2016). https://doi.org/10.1088/1674-1137/40/9/091002
39. P.H. Chen, Z.Q. Feng, F. Niu et al., Effect of isospin diffusion on the production of neutron-rich nuclei in multinucleon transfer reactions. Eur. Phys, J. A **53**, 95 (2017). https://doi.org/10.1103/PhysRevC.97.034609
40. Z.Q. Feng, G.M. Jin, J.Q. Li, Influence of entrance channels on the formation of superheavy nuclei in massive fusion reactions. Nucl. Phys. A **836**, 82 (2010). https://doi.org/10.1016/j.nuclphysa.2010.01.244
41. P.H. Chen, F. Niu, Y.F. Guo et al., Nuclear dynamics in multinucleon transfer reactions near Coulomb barrier energies. Nucl. Sci. Tech **29**, 185 (2018). https://doi.org/10.1007/s41365-018-0521-y
42. H. Feldmeier, Transport phenomena in dissipative heavy-ion collisions: the one-body dissipation approach. Rep. Prog. Phys. **50**, 915–994 (1987). https://doi.org/10.1088/0034-4885/50/8/001
43. Z.Q. Feng, Nuclear dynamics and particle production near threshold energies in heavy-ion collisions. Nucl. Sci. Tech **29**, 40 (2018). https://doi.org/10.1007/s41365-018-0379-z